Wetting of a Fiber Bundle in Fibrous Structures

DAVID LUKAS

Technical University of Liberec
461 17 Liberec, Czech Republic

and

NING PAN

Division of Textiles and Clothing
Biological and Agricultural Engineering Department
University of California
Davis, CA 95616

In this paper we dealt with the problem of wetting and ascending of a liquid along a fiber bundle. Two issues are first addressed including the criterion for complete wetting of the fiber bundle and the ascension liquid profile on a partially dipped vertical fiber bundle. Both topics are studied theoretically by deriving a mathematical theory by which predictions are generated and important parametric analyses are carried out. Further, a 3D Ising model is used for computer modeling to simulate the fiber wetting and liquid ascending processes on a partially dipped single fiber. The significance and potential applications of the study are also summarized.

1. INTRODUCTION

Study of fiber wetting behavior is critical in prediction of properties and performance of fibrous structures such as fiber reinforced composites and textiles. On the other hand, the most often studied cases in physics for wetting phenomena are the wetting of solid planes (1–5). Compared to the plane wetting situation, the wetting of a fiber exhibits some unique features due to the inherent fiber curvature (6, 7). Brochard (7), for instance, derived the critical spreading parameter S_{CF} for complete fiber wetting transition and proved that this parameter is greater than that for a plane of the same liquid/solid system. It means liquids are more willing to wet planes than to individual fibers of the same material, due to the cylindrical shape of a fiber.

However, in spite of this higher inertia of wetting process of individual fibers, one of the best known and most frequently used materials for liquid absorption is fiber assemblies. Their excellent behavior during wetting processes could be intuitively explained by the capillary effect due to their collectively large inner surface area, but a more quantitative theory of fiber assembly wetting at the microscopic level has yet to be fully developed.

We attempt in this paper to extend the approach presented by Brochard (7, 8) and Bacri (6, 9) obtained for single fiber wetting, to the spreading of a liquid along a fiber bundle, which is defined as an arrangement of several fibers parallel to each other as shown in *Fig. 1*. We will derive the critical spreading parameter SCB for a fiber bundle in comparison with that of either plane or a single fiber. We then develop a theory to predict the ascension profile of a liquid along a vertical fiber bundle. The nonlinear relationship between the liquid profile and the bundle properties observed experimentally will be predicted by the theoretical tool. Further we will introduce a 3D Ising model, which is an extension of the 2D model developed by us before (10), to simulate much more realistically the wetting process of fiber assemblies. Yet as the first step, we only predict in this paper the wetting behavior of a single fiber dipped partially in a liquid pool. More comprehensive results from the 3D Ising modeling, and an experimental verification will be reported in a following paper.

2. COMPLETE WETTING OF FIBER BUNDLES

We will restrict our discussion to the case of nonvolatile liquids. According to Brochard (7) we define the complete wetting of a single fiber of radius b as the state when the fiber is covered by a liquid "manchon" as this liquid geometry is less energy demanding than the nearly spherical droplet sessile on the fiber. Let us denote γ_{SO}, γ_{SL} and γ the surface tensions of the solid fiber, the solid/liquid interface, and the liquid (or liquid/air). The liquid film thickness in

the manchon is represented by a parameter e. This liquid manchon formation occurs when the so-called Harkinson spreading parameter S (7) defined as

$$S = \gamma_{SO} - \gamma_{SL} - \gamma \tag{1}$$

reaches the critical value S_{CF} derived in (7).

$$S_{CF} = \frac{e\gamma}{b}. \tag{2}$$

That is, the fiber will be covered by liquid manchon in the case of the following inequality

$$S > S_{CF} = \frac{e\gamma}{b}. \tag{3}$$

Compared to the wetting of planes, the wetting of individual fibers is a more energy-consuming process according to Young Equation (8, 11), as for complete wetting of a flat solid it only requires

$$S > 0. \tag{4}$$

In other words, for a plane, the critical spreading parameter S_{CP} holds

$$S_{CP} = 0. \tag{5}$$

From *Eqs 3* and *4* we see that it is obvious that liquids will wet a solid plane more promptly than wet a fiber.

Next, let us examine the case of a fiber bundle formed by n parallel fibers as seen in *Fig. 1*, each with a radius b. Two different types of liquid body geometry caused by the liquid/fiber bundle interactions are possible, just like in the individual fiber cases (7) mentioned above. The first is the drop-like geometry shown in *Fig. 1a* and the second one is the manchon shape in *Fig. 1b*. Let us focus on the second, less energy demanding, case and assume the manchon is a cylindrically symmetric liquid body with an equivalent radius R as shown in *Fig. 2*.

The Equilibrium configurations of limited amounts of liquid in horizontal assemblies of parallel cylinders have been introduced and described in detail by Princen (12–14). The criterion of complete wetting of a vertical fiber bundle dipped partially in a liquid will be derived here by the comparison of the surface energy W_m of such a manchon liquid geometry with the surface energy W_b of a dry fiber bundle. For a length L of the dry fiber bundle,

$$W_b = 2\pi bnL\gamma_{SO} \tag{6}$$

Whereas the same length of liquid formed manchon on the fiber bundle has the surface energy

$$W_m = 2\pi bnL\gamma_{SL} + 2\pi RL\gamma \tag{7}$$

That is, the energy W_m is composed of both terms of solid/liquid interface and liquid/air interface. The complete wetting sets in when the wet state of the system is energetically more favorable compared with the dry one, i.e., $W_b > W_m$. Or from previous equations

$$\gamma_{SO} - \gamma_{SL} - \frac{R.\gamma}{n.b} > 0 \tag{8}$$

Inserting Harkinson spreading coefficient from *Eq 1* into *Eq 8* yields

$$S > \frac{R - n.b}{n.b}\gamma \tag{9}$$

So the critical value S_{Cb} for the complete wetting of the bundle system is

$$S_{Cb} = \frac{R - n.b}{n.b}\gamma \tag{10}$$

The radius of the manchon R could be smaller than the total sum of fibers radii nb. *Figure 2* shows us such an example when the cross-section of the seven-fiber bundle is covered by a liquid cylinder. The value of S_{Cb} is clearly only $-4/7\ \gamma$.

The above results show that it is highly probable for such a solid/liquid system in which, on one hand, the liquid will wet a solid plane but not a single fiber, and on the other hand, the liquid will wet a fiber bundle, even before it does the solid plane. This of course is attributable to the familiar capillary mechanism. However, the above simple analysis also explains the excellent wetting properties of a fiber mass in terms of energy changes; the consequence of collective behavior of

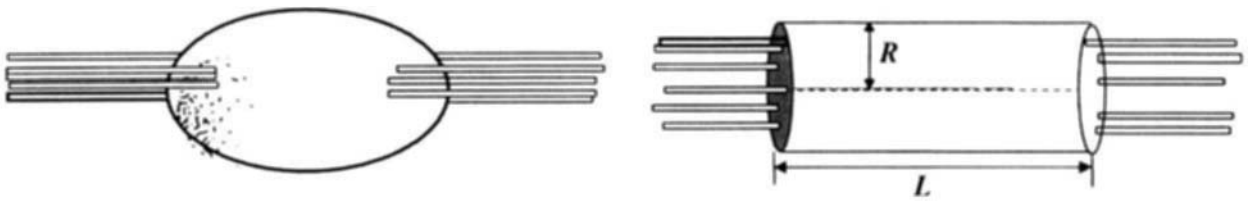

Fig. 1. Two different types of a liquid body, droplet-like (a) and manchon (b), are the consequence of liquid/fiber-bundle interaction. The manchon has a diameter R and length L.

$$n = 7$$
$$R = 3b$$

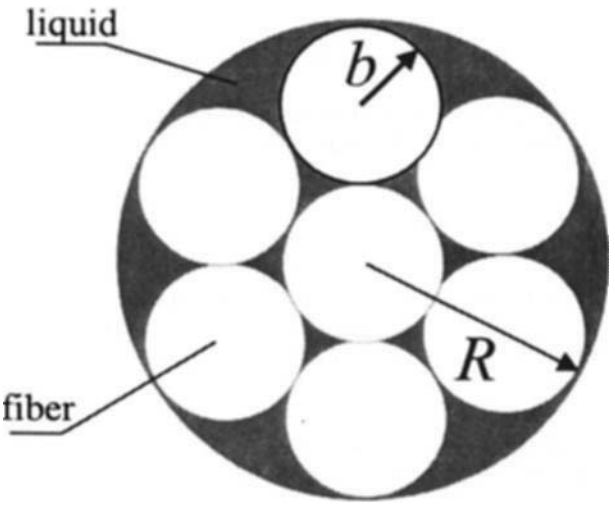

Fig. 2. The cross-section of the liquid manchon that covers the narrow bundle of seven fibers, each of the radius b. The manchon radius is denoted R and obviously R = 3b.

fibers in the bundle allows the manchon energy W_m increasing more rapidly with the fiber number n in the bundle than the dry bundle energy W_b.

3. SHAPE OF LIQUID BODY SPREADED ON A FIBER BUNDLE

Brochard's deduction (7) of a liquid body profile in wetting regime for a single fiber is easily extendible to a small bundle of parallel fibers with the assumption of axial symmetry of the sessile liquid body. Our goal here is to obtain the relationship between the liquid body profile Φ(x) measured from the bundle to the liquid/air interface. The equivalent radius of the fiber bundle is denoted above as R, and the bundle is vertically dipped into the liquid as shown in *Fig. 3*.

The base for the derivation is the equilibrium of the projections onto the bundle axis x of the capillary forces (7). The particular force projections taking part in the equilibrium include the one spreading the liquid on a fiber caused by γ_{SO}, parallel with bundle axis, the force due to the fiber/liquid surface tension γ_{SL}, parallel with but opposite to γ_{SO}, and the third one in the direction with an angle θ from the x axis representing the liquid surface tension γ as illustrated in *Fig. 3*.

In the Laplace force regime, the equilibrium of the capillary forces acting on the liquid spread on the fiber bundle is

$$2\pi n.b\gamma_{SO} = 2\pi n.b\gamma_{SL} + 2\pi(\Phi(x) + R)\cos\theta. \quad (11)$$

In our consideration we neglect the gravity effects, since addition of a gravitational term into *Eq 11* will make it mathematically unsolvable. Yet it has been indicated (5) that for relatively short fibers (≤ 10 cm), the effects of the gravitational force are negligible. Furthermore, effect of the gravity will be considered in a 3D Ising model presented in next section.

Using the following relations

$$\cos\theta = \frac{1}{\sqrt{1 + \tan^2\theta}} \quad (12)$$

and

$$\tan\theta = \frac{d\Phi(x)}{dx} = \Phi'(x) \quad (12b)$$

Equation 11 can be rewritten into the form of nonlinear differential *Eq 13*.

$$\frac{R + \Phi(x)}{\sqrt{1 + \Phi'^2(x)}} = np \quad (13)$$

where p is a system constant

$$p = b\left(\frac{S}{\gamma} + 1\right) \quad (14)$$

The solution of *Eq 13* is the function Φ(x) that represents the equilibrium profile of the liquid mass clinging on to the fiber bundle

$$\Phi(x) = np\cosh\left(\frac{x - x_o}{np}\right) - R \quad (15)$$

where x_o specifies the peak point of the macroscopic meniscus. We can set $x_o = 0$ so that

$$\Phi(x) = np\cosh\left(\frac{x}{np}\right) - R \qquad 0 \le x < \infty \quad (15b)$$

where x is the height along the fiber bundle but measured from the top of the liquid profile as shown in *Fig. 3*. It is clear that in order to maintain the solution

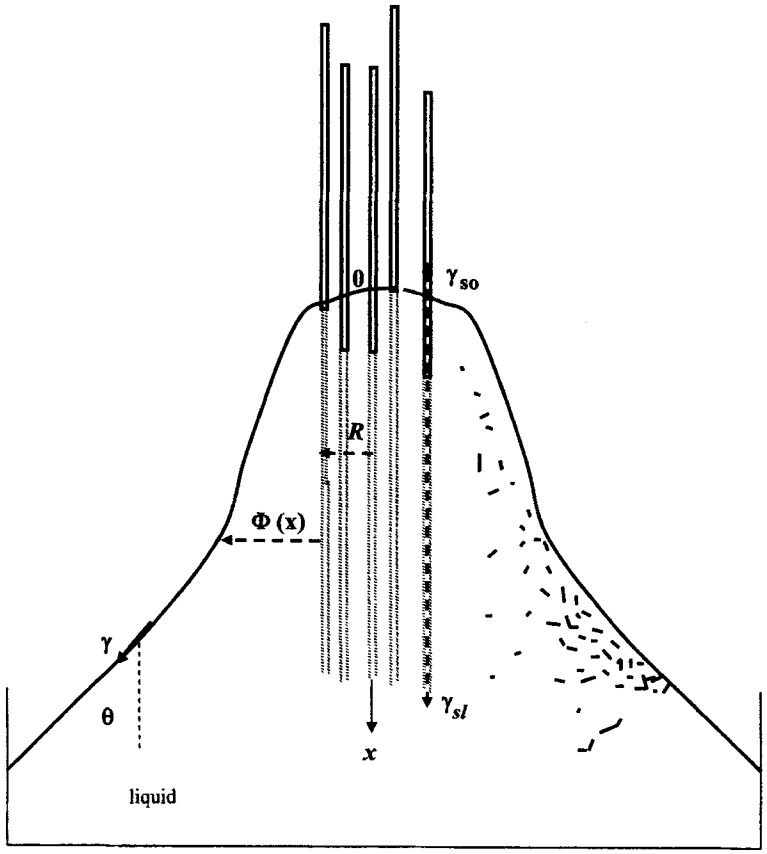

Fig. 3. The liquid profile Φ(x) and surface tensions along a fiber bundle.

of the equation meaningful, i.e., $\Phi(x) \geq 0$, first there has to be $p > 0$, which translates into

$$\frac{S}{\gamma} > -1 \quad \text{or} \quad \gamma_{SO} > \gamma_{SL} \tag{16}$$

The physical implication of this inequity is obvious that a necessary condition for wetting a fiber bundle is that the surface tension of the fiber γ_{SO} has to be greater than the fiber/liquid surface tension γ_{SL}.

Furthermore, from *Eq 15b*, we can see that there is a criterion in determining the equivalent fiber bundle radius R. Since $\Phi(x) \geq 0$ so that

$$R \leq np \cosh\left(\frac{x}{np}\right) \tag{17}$$

As $\cosh(x)$ achieves the minimum when $x = 0$, and $\cosh(0) = 1$, we have the limit for R

$$R \leq np = nb\left(\frac{S}{\gamma} + 1\right) \tag{18}$$

In the case $R > np$, the mathematical solution of $\Phi(x)$ no longer has physical meaning. Shown in *Eq 18*, the spacing between fibers in the bundle is limited by the spreading ratio S/γ. By using *Eq 16*, i.e. $S/\gamma > -1$, the minimum value of the bundle radius $R = R_{min} > 0$.

Furthermore, when $x = 0$, and $\cosh(0) = 1$, then *Eq 15b* gives $\Phi(0) = np - R$. It means that according to *Eq 18*, beneath the liquid meniscus with the *hyperbolic cosin* shape, there exists a microscopic liquid film on the fiber bundle, whose thickness is

$$\Phi(0) = np - R > 0 \tag{19}$$

This may indicate that at the point where the liquid mass profile starts, i.e.,, $x = 0$, the liquid first coats the fiber bundle with a thin layer of thickness $np - R$. We need to verify this conclusion in latter study, in view of the ignorance of the gravitational effects in the analysis.

Considering the upper limit for the bundle radius $R = np$ in *Eq 18*, the lower limit $\Phi_o(x)$ of the liquid profile $\Phi(x)$ in *Eq 15b* can be expressed in terms of the Harkinson spreading parameter S and the liquid surface tension γ:

$$\Phi_o(x) = nb\left(\frac{S}{\gamma} + 1\right)\cosh\left(\frac{x}{nb\left(\frac{S}{\gamma} + 1\right)}\right) - nb\left(\frac{S}{\gamma} + 1\right) \quad 0 \leq x \leq \infty \tag{15c}$$

That is, $\Phi_0(x)$ is a function of the height x, the spreading ratio S/γ reflecting the surface properties of liquid, the fiber, and the liquid/fiber interfacial property, as well as the fiber parameters *nb*, as plotted in *Fig. 4* based on *Eq 15c*.

In general, $\Phi_0(x)$ increases with x when other parameters are given. The effect of the number of fibers in a bundle is seen in *Fig. 4a* where a small bundle (small n value) will have a greater amplitude of $\Phi_0(x)$ at a given position x.

The fiber radius b has the similar influence on $\Phi_0(x)$, i.e., $\Phi_0(x)$ increasing with b for a given x, except that it also determines the maximum value, $\Phi_m(x)$ and the maximum height x_m as seen in *Fig. 4b*; when b is smaller, the $\Phi_m(x)$ value as well as x_m will be accordingly smaller. *Figure 4c* shows the same thing can be said about the effect of the spreading ratio S/γ; a smaller ratio S/γ results in a smaller $\Phi_m(x)$ and x_m.

Once again, the solution to *Eq 15* has a shortcoming resulted from the exclusion of gravity in the analysis. The consequence is an asymptotical behavior of $\Phi(x)$ that does not converge to the flat horizontal surface of the liquid source perpendicular to the fiber bundle.

4. 3-DIMENSIONAL ISING MODEL

Besides the mathematical theory adopted in last section, we have also carried out a computer simulation of fiber wetting process using the 3D Ising model, an extension of our 2D Ising model in (10). The goal of the simulation is to model the entire equilibrium process of the system where liquid-liquid, liquid-air, air-air and liquid-gravitation interactions are all considered. This work employs the 3D Ising Model with Kawasaki spin exchange dynamics, and the iteration procedure in the computer algorithm is based on a method of finding a global minimum of the system's Hamiltonian.

The 3D Ising model consists of a 3D cubic lattice. Distances in the lattice are measured in the size of a cell known as the lattice unit (*lu*). Each of the lattice cells represents liquid, air or fiber segment according to the following rules.

If cell i is occupied by one of the fluids (air or the liquid), the cell is designated with an Ising variable σ_i that acquires two alternating spin values, i.e. $\sigma_i \in \{+1, -1\}$. The distribution of the two different values of σ spins forms the so called binary mixture (1). The spin $\sigma_i = +1$ indicates the cell is filled with the liquid, and $\sigma_i = -1$ filled with air, i.e., an empty cell. Likewise, the Ising variable related to fiber is designated as $S_i \in \{0, +1\}$, $S_i = +1$ is used for a cell occupied by the fiber material, and otherwise $S_i = 0$. A cell must be occupied by at least one substance, be liquid $\sigma_i = +1$, air $\sigma_i = -1$ or fiber $S_i = +1$, as depicted in *Fig. 5*. For simplicity, $S_i = 0$ is often omitted. The spin variables σ and S can overleap in each lattice cell, meaning that a cell may be occupied simultaneously by the fiber material along with one type of the fluids of either the liquid or air (wet or dry fiber).

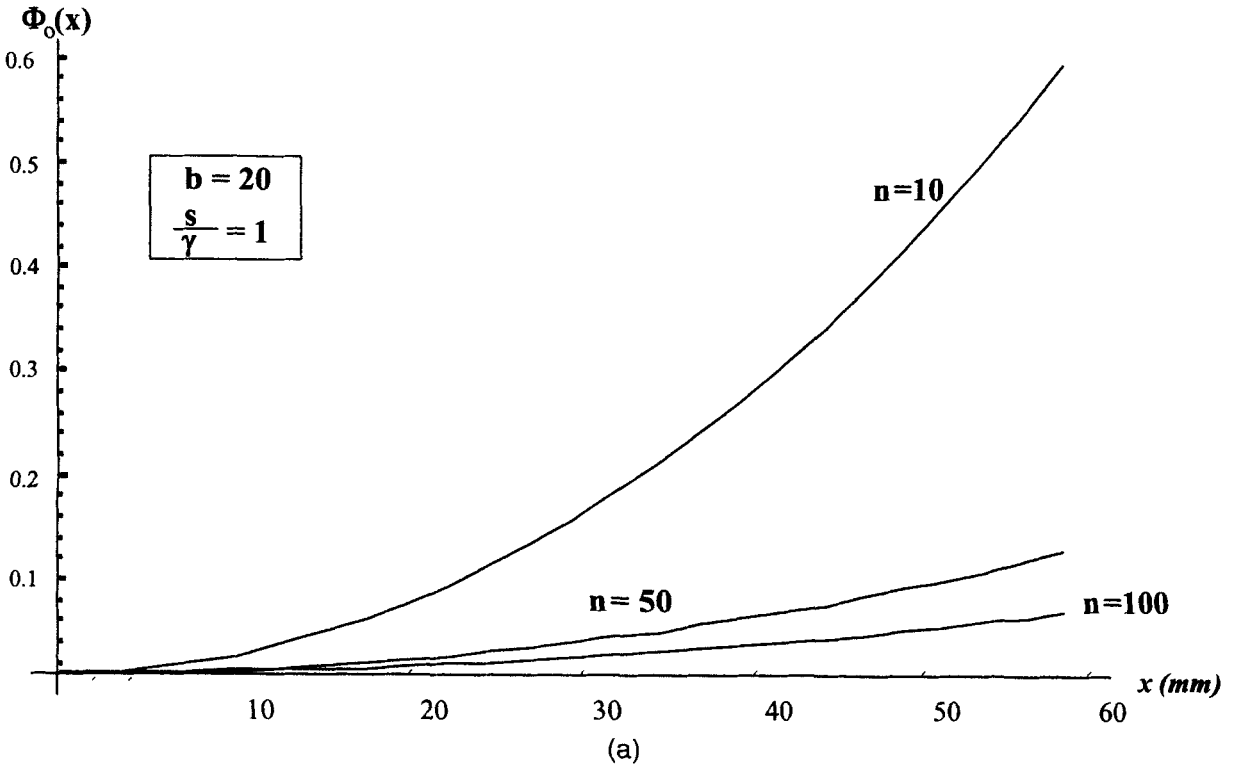

Fig. 4. Factors affecting the lower boundary $\Phi_0(x)$ of ascension liquid bodies (a). The effects of bundle size (number of fibers) n; (b). The effects of fiber radius b; (c). The effects of the spreading ratio S/γ.

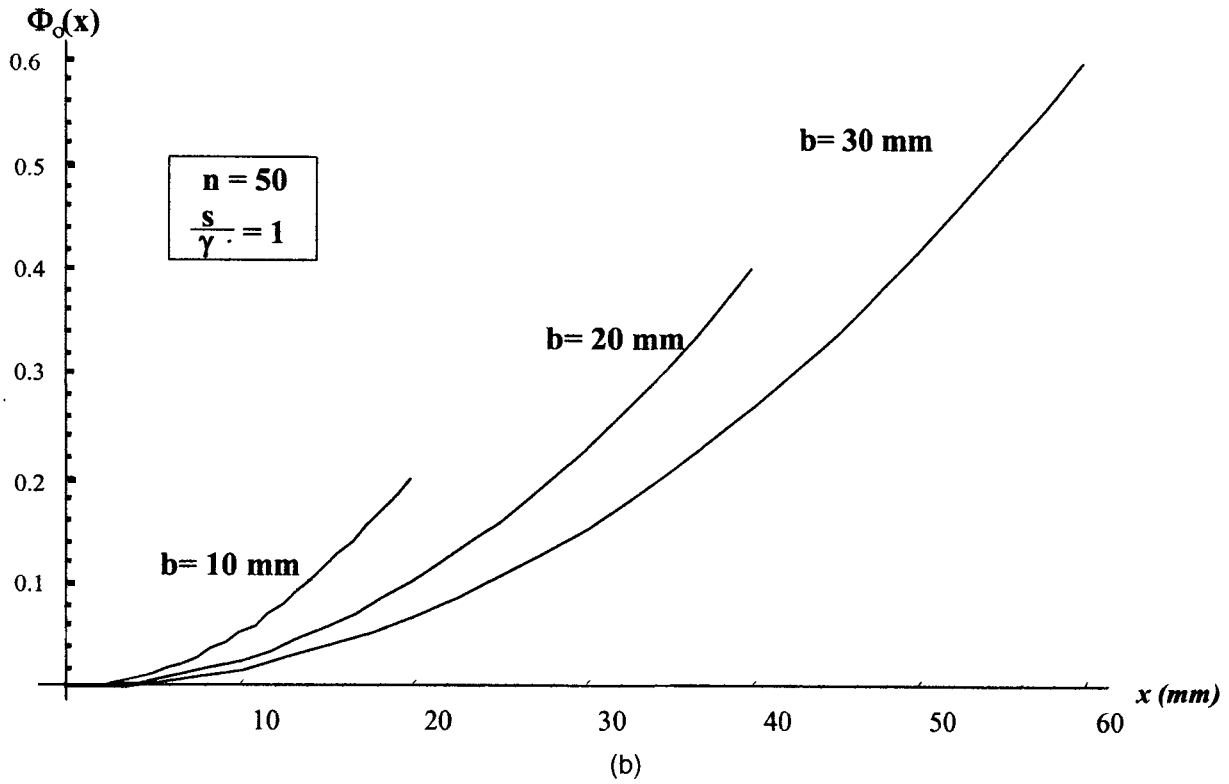

(b)

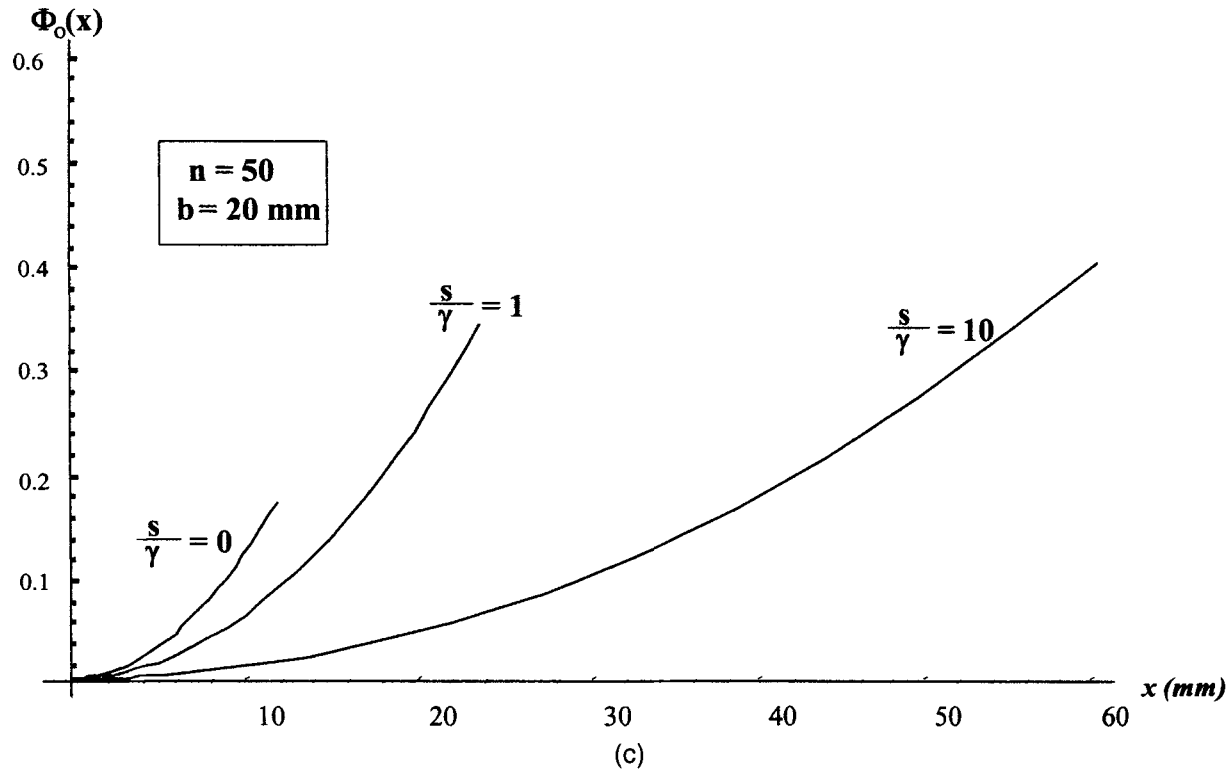

(c)

Fig. 4. Continued.

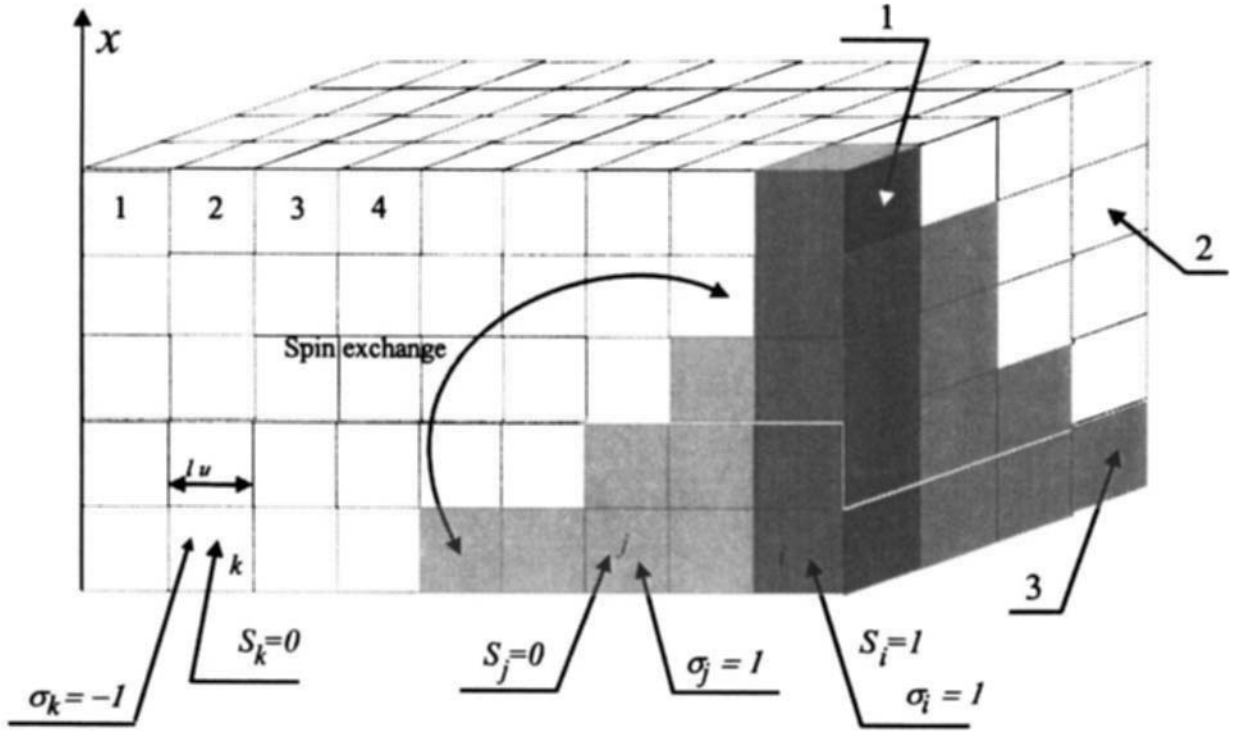

Fig. 5. The cubic lattice of the Ising model contains liquid (3), air (2) and fiber (1) cells. Distances in the model are measured in lattice units (lu).

A binary mixture cell of the Ising variable thus defined has to interact with its neighbor cells in the lattice. A complete assembly of the neighborhood in 3D case consisting of 26 cells that surround the one in the center is called the neighborhood supercube as shown in *Fig. 6*.

Three different kinds of interactions are existent in the model. For two cells i and j filled with fluids as the Ising variable σ_i and σ_j, the energy generated through the cell interactions is

$$H_1 = - C_1 \sigma_i \sigma_j \qquad (20a)$$

where C_1 is a positive coefficient. So when both Ising variables have the same sign, meaning they are both filled with the same fluids (liquid or air), then the interaction energy $H_1 < 0$; the two cells attract each other and there is cohesive energy. If the two cells have the opposite signs, the energy, $H_1 > 0$, is repulsive due to liquid surface tension. An adhesive case occurs between two cells, one with the Ising variable σ_i, another with $S_j = 1$, that is, between a fluid cell and a fiber cell so that

$$H_2 = - C_2 \sigma_i S_j \qquad (20b)$$

where again C_2 is a positive coefficient. When $\sigma_i = +1$, the adhesion energy $H_2 < 0$; otherwise $H_2 > 0$.

The last kind of interaction in the model is the interaction of a liquid cell with the external gravitation field that the liquid has to overcome in order to climb along a fiber. The gravitation energy is linearly proportional to the height or the coordinate $x(i)$ of the liquid cell. The corresponding energy contribution is therefore

$$H_3 = - C_3 x(i) \delta(\sigma_i - 1) \qquad (20c)$$

where C_3 is also a positive coefficient, and δ is the Dirac function to eliminate the cells filled with air.

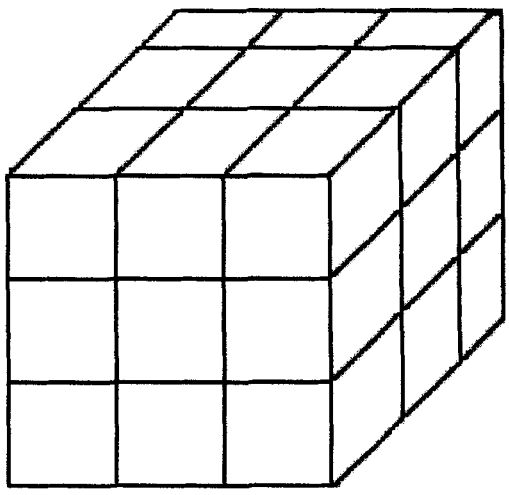

Fig. 6. The neighborhood of a chosen cell has a shape of a supercube. The cell in the center of the supercube is surrounded by 26 neighboring cells.

The Hamiltonian H of the whole system hence consists of three terms, each representing the total sum of the energy contribution over all related lattice cells and their neighbors.

$$H = \sum H_3 - \sum H_1 - \sum H_2 \tag{21a}$$

or

$$H = \sum_{i=1}^{N} C_3 x(i)\delta(\sigma_i - 1) + \sum_{i=1}^{N}\sum_{j=1}^{Neighbours} C_1\sigma_i\sigma_j + \sum_{i=1}^{N}\sum_{j=1}^{Neighbours} C_2\sigma_i S_j \tag{21b}$$

For the three terms summed over the individual cells, each couple of interacting cells is added only once. The second and third sums in the RHS of *Eq 21b* understandably go through the neighboring cells, where N denotes the total number of cells in the 3D lattice.

The minimization of the system Hamiltonian H is based on descent steps caused by spin exchanges that obey the Kawasaki spin dynamics (1). The procedure conserves the number of liquid cells in the model. Let us consider the Ising model as a thermodynamics system connected with a thermodynamics reservoir, and energy exchange can occur between them. The system together with the reservoir forms a canonical assembly that is governed by the Boltzmann distribution of the state probability ratio (5, 10), i.e.

$$\frac{P(H_a)}{P(H_b)} = \Lambda = \exp\left(-\frac{\Delta H}{\tau}\right) \tag{22}$$

where the parameter τ is proportional to the absolute temperature which may be chosen as an input variable in the simulation process to examine the temperature effects, and Λ is the ratio of $P(H_a)$ and $P(H_b)$. $P(H_k)$, (k = a and b) is the probability that the system exists with configuration associated with energy H_k. Λ is then a measure of the likelihood for the system to change its configuration, through spin exchange from the state with energy H_a to the state with energy H_b. The energy difference $H_a - H_b$ denoted by ΔH is the difference of the total system energy before and after the spin exchange.

In Kawasaki dynamics, two randomly chosen spins σ_i and σ_j of different values +1 and −1 are considered. The system Hamiltonians H_a and H_b are calculated for cases before (H_a) and after (H_b) the spin exchange. A random number r is then chosen from the interval (0, 1) as spin exchange probability. In the case r is less than the energy barrier given by the Boltzmann law

$$r < \Lambda = \exp\left(-\frac{\Delta H}{\tau}\right) \tag{23}$$

these two spins will exchange their position.

The implication of the connection between the energy state and the spin exchange probability in *Eq 23* is very important. Since Λ is just a ratio of probabilities, it can be greater than 1 as evident in the equation. But if $\Lambda > 1$, then $\Delta H < 0$ or $H_b > H_a$. This means from *Eq 22* the probability $P(H_a)$ of the system remaining at the state with energy H_a is greater than that at the state with energy H_b. So the spins exchange will not occur regardless of the r value. So in that sense, we can say that *Eq 23* is only a necessary but not sufficient condition for spin exchange. A more detailed discussion on this can be found from our previous paper (10).

During the iteration procedure (step by step σ spin exchanges of the computer simulation), the Hamiltonian descending is monitored and the simulation is terminated in the case when a steady state of the system energy is reached. The fiber Ising variables S's obviously remain in their assigned original positions during the whole simulation.

Figure 7 shows us the computer simulation output that models the equilibrium shape of a liquid body in interaction with a partially dipped fiber. The simulation was carried out on a 20 *lu* × 20 *lu* × 30 *lu* lattice.

From the above analysis, several advantages can be found about the proposed approach. First, the Ising model can describe a complex physical phenomenon in a very simple binary form, yet still able to account for all the mechanisms involved and yield realistic results. This makes the model a very attractive, practical and powerful tool to study the phenomenon of liquid transport in fiber network. In other words, the very complex wetting process can be realistically simulated without employing intricate mathematical operations.

Also, the constants associated with the energy terms C_i's have clear physical meanings, and they in fact represent the properties of the media involved. Thus, by adjusting the values of these constants, we can carry out a series of parametric study of the influences of these properties on a specific problem under investigation.

The proposed simulation technique will enable us to obtain information about the nature and mechanisms of the fiber mass wetting behavior. All the important interactions and factors have been included in terms of the energies they contribute to the whole process. The results enable us to study some practical issues and provide powerful tools for understanding and monitoring the wetting performance of fibrous products.

5. CONCLUSIONS

First of all, the results in this study have explained the excellent wetting properties of fiber mass as the consequence of collective behavior of individual fibers known as the capillary phenomenon, even though a single fiber is relatively difficult to wet because of the inherent shape curvature.

For a wetted fiber bundle, the lower boundary $\Phi_0(x)$ of the liquid profile of the ascension liquid from the equivalent bundle surface is a function of several parameters besides the height x. The size (number of fibers) of the fiber bundle n has no influence on the range of the profile, and it only changes the maximum

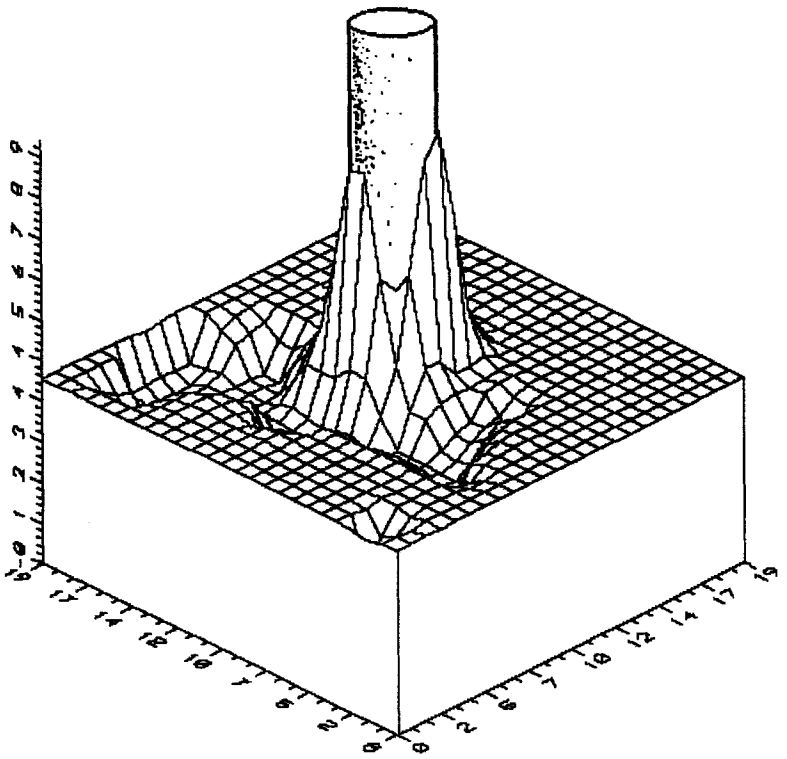

Fig. 7. 3-D equilibrium liquid body shape along a single fiber as the consequence of liquid-air-fiber-gravitation interactions.

amplitude of the liquid profile $\Phi_m(x)$. For a larger bundle with more fibers, the liquid profile becomes thinner, i.e., indicated by a smaller $\Phi_o(x)$ value at a given height x. Whereas the fiber radius b affects both the range x_m and the maximum amplitude $\Phi_m(x)$ of the profile. When other variables are fixed, a thicker fiber will lead to a greater range x_m but a smaller $\Phi_m(x)$.

The next important parameter is the spreading ratio S/γ. It has been proved here that in order to wet a fiber bundle, i.e., the liquid profile thickness $\Phi(x) > 0$, there is a minimum value $S/\gamma > -1$, or $\gamma_{SO} > \gamma_{SL}$. That is, the surface tension of the fiber bundle has to be greater than that of the fiber/liquid interface.

Furthermore, the Ising model can describe a complex wetting phenomenon in a very simple binary form, yet still able to account for all the mechanisms involved, to yield realistic results, and to conduct parametric investigations. This makes the model a very attractive, practical and powerful tool to study the phenomenon of liquid transport in fibrous systems, and the very complex wetting process can be realistically simulated without employing intricate mathematical operations.

6. ACKNOWLEDGMENT

This work was partially supported by the Research Center-TEXTIL (LN00B090) of the Technical University of Liberec.

REFERENCES

1. D. B. Abraham and C. M. Newman, *Lecture Notes in Physics*, **354**, 13 (1988).
2. C. Andrieu and C. Sykes, *et al. Langmuir*, **10**, 2077 (1994).
3. F. Brochard and E. Raphael, *et al., Comptes Rendus De L Academie Des Sciences Serie Ii Fascicule B-Mecanique Physique Chimie Astronomie*, **321**, 367 (1995).
4. P. G. De Gennes, *Rev. Mod. Physics*, **57**, 827 (1985).
5. S. S. Manna, H. J. Hermann, and D. P. Landau, *J. Statist. Physics*, **66**, 1155 (1992).
6. J. C. Bacri, R. Perzinski, and D. Salin, *Lecture Notes in Physics*, **354**, 1 (1988).
7. F. Brochard, *J. Chem. Phys.*, **84**, 4664 (1986).
8. F. Brochard and J. M. Dimeglio, *et al., Comptes Rendus De L' Academie Des Sciences Serie Ii-Mecanique Physique Chimie Sciences De L' Univers Sciences De La Terre*, **311**, 1473 (1990).
9. J. C. Bacri, R. Perzinski, D. Salin, and H. O. Tourin, *Europhysics Lett.*, **5**, 547 (1988).
10. D. Lukas, N. Pan, and E. Glazyrina, *J. Textile Institute*, **88**, Part 1, 149 (1997).
11. T. Young, *Philos. Trans. R. Soc. London*, **95**, 65 (1805).
12. H. M. Princen, *J. Colloid and Interface Science*, **30**, 69 (1969).
13. H. M. Princen, *J. Colloid and Interface Science*, **30**, 359 (1969).
14. H. M. Princen, *J. Colloid and Interface Science*, **34**, 171 (1970).